A real-time 2D PEMFC model for fuel cell vehicle hardware-in-the-loop applications

Pierre Massonnat
IEEE student member
IRTES-SET,
University of Technology
of Belfort Montbeliard,
Belfort, France
pierre.massonnat@utbm.fr

Fei Gao
IEEE member
IRTES-SET,
University of Technology
of Belfort Montbeliard,
Belfort, France
fei.gao@utbm.fr

David Bouquain
IRTES-SET,
University of Technology
of Belfort Montbeliard,
Belfort, France
david.bouquain@utbm.fr

Abdellatif Miraoui
IEEE senior member
IRTES-SET,
University of Technology
of Belfort Montbeliard,
Belfort, France
abdellatif.miraoui@utbm.fr

***Abstract*—In this paper, a real-time 2D PEMFC multi-physiques model is developed for fuel cell vehicle simulation purpose. For the consideration of real time model performance, an extrapolation method of a 1D channel pressure model into a 2D pressure map is used in the presented model. The developed PEMFC model is validated with experimental test. From the 2D modeling approach, different channel configuration types are also compared and discussed. The presented PEMFC model is developed for real-time fuel cell vehicle simulation and hardware-in-the-loop applications.**

I. Introduction

Fuel cell is a chemical/electrical energy conversion device. Among different type of fuel cells, proton exchange membrane fuel cell shows its great interest in vehicle applications due to its relatively fast start time. Compared to other conventional energy conversion devices, such as internal combustion engine (ICE), a higher energy conversion efficiency can be achieved by fuel cells, because the fuel cell can directly convert chemical energy into electricity. In addition, the byproduct of the fuel cell is only water, the emission of green house gas can be thus eliminated for vehicles running with fuel cells. In order to evaluate the fuel cell vehicle performance, a fuel cell model is needed.

In the literature, a PEM fuel cell electrochemical model has been developed in [1]. However, the fluidic phenomena is not considered. A 1D multi-physiques real time PEMFC model has been presented in [2]. Due to its 1D approach, the fluid channel configurations are not taken into account. A 2D steady state model has been developed in [3], but the model is not suitable for real time simulations. Many 3D models have been presented in [4], [5] and [6] but all these models depend on commercial finite element software. A complex mathematics multi-physiques model have been developed in [7] and later a more simple one in [8]. A study of PEMFC model parametric sensitivity has been shown in [9]. For fuel cell vehicle on-board hydrogen generation, a PEM electrolyser model and a PEM fuel cell model have also been shown in [10].

Aimed to give a powerful simulation model for PEM fuel cell in vehicles and to understand the associated physical phenomenon, a real-time 2D PEMFC model is developed in this paper. This model is suitable for real-time hardware-in-the-loop applications. The paper is organized as follow: the multi-physiques PEMFC model is introduced in the first part. A presentation of the extrapolation method for 2D modeling approach is given in the second part of the paper. At last, the experimental validations of the model are presented and the results are discussed.

II. PEM fuel cell model

A. Electrochemical model

The potential of the fuel cell is determined by :

$$U_{cell} = U_{NERNST} - U_{act} - R_{mem} \times i \tag{1}$$

Where U_{NERNST} is the thermodynamic potential in V, U_{act} is the activation loss, R_{mem} is the membrane resistance in Ω and i is the fuel cell current in A.

1) Thermodynamic potential: The thermodynamic potential of a PEMFC is determined by the Nernst law in V:

$$\begin{aligned} U_{NERNST} &= 1.23 - 0.85 \times 10^{-3}(T - 298.15) \\ &\quad +4.3085 \times 10^{-5} T \left(ln\left(P_{H_2}\right) + \tfrac{1}{2} ln\left(P_{O_2}\right) \right) \end{aligned} \tag{2}$$

Where P_{H_2} and P_{O_2} are the respectives hydrogen and oxygen partial pressure in atm.

2) Activation loss: In a PEMFC, the Activation loss can be calculated by Butler-Volmer law :

$$i = i_0 \left(exp\left(\frac{\alpha n F}{RT} U_{act} \right) - exp\left(\frac{-(1-\alpha) n F}{RT} U_{act} \right) \right) \tag{3}$$

Where α is electrochemical reaction parameter, n is the number of exchanged electrons in electrochemical reaction and i_0 the electrode reference exchange current in A.

3) Membrane resistance: The membrane resistivity in $\Omega \cdot m$ can be determined by the empirical model proposed by Springer found in [11], [12] and [13] :

$$r_{mem} = \begin{cases} \frac{1}{0.1879} exp\left(1268\left(\frac{1}{T} - \frac{1}{303}\right)\right) & \text{if } \lambda \leq 1 \\ \frac{1}{0.5139\lambda - 0.326} exp\left(1268\left(\frac{1}{T} - \frac{1}{303}\right)\right) & \text{if } \lambda > 1 \end{cases} \tag{4}$$

Where membrane water content λ is the water content of the membrane.

The λ is expressed as:

$$\lambda = \begin{cases} 0.043 + 17.81a_{mem} - 39.85a_{mem}^2 + 36.0a_{mem}^3 \\ \text{if } a_{mem} < 1 \\ 14 + 1.4(a_{mem} - 1) \text{ if } a_{mem} \geq 1 \text{ and } a_{mem} < 3 \\ 16.8 \text{ if } a_{mem} \geq 3 \end{cases} \tag{5}$$

Where a_{mem} is the water activity of membrane.

From the equations above, the membrane resistance R_{mem} is then determined by :

$$R_{mem} = \frac{r_{mem}\delta_{mem}}{A} \tag{6}$$

Where A is the fuel cell section area and δ_{mem} the membrane thickness in m^2 and m respectively.

B. Mass transfer model

A 1D mass transfer model is developed first in this section to determinate the variations of mass transfer parameters in fuel cell channels. After that, the 1D model is then exported to a 2D matrix by linear interpolation method according to channel configuration, in order to obtain a 2D model with the consideration of channel geometry.

1) In the channel: The variation of gas pressure in channel is due to two main phenomena : the friction of gas in the channel and the diffusion from channel to the gas diffusion layer.

The gas pressure drop due to the friction can be modeled by Darcy-Weisbach's law [2] :

$$\Delta P = f_D \rho \frac{L}{D_h} \times \frac{u^2}{2} \tag{7}$$

Where f_D is the Darcy's parameter in $kg \cdot m^{-1} \cdot s^{-2}$, D_h is the hydraulic diameter in m, L is the length of channel in m. ρ is the gas density in $kg \cdot m^{-3}$, u the gas average speed in $m \cdot s^{-1}$.

The Darcy's parameter can be calculated from:

$$f_D = \frac{64}{Re} \tag{8}$$

Where Re is the Reynold number.

The hydraulic diameter is calculated by :

$$D_h = \frac{4S_{cha}}{P_{cha}} \tag{9}$$

Where S_{cha} is the channel surface area and P_{cha} the perimeter of the section of the channel.

The gas pressure drop due to the diffusion from channel to the gas difusion layer can be determined by mass conservation law :

$$\rho_{in} S_{cha} u_{in} - \rho_{out} S_{cha} u_{out} - N = 0 \tag{10}$$

Where N is the mass flow rate across Diffusion layer in $kg \cdot s^{-1}$.

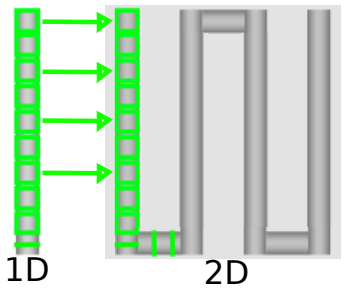

Fig. 1. Two dimensional pressure interpolation

2) In Diffusion layer: The first law of Fick is used to calculate the concentration gradient gaz between channels and gas reaction sites :

$$N = -D_{i,j}^{eff} \frac{\partial \rho}{\partial x} \Longrightarrow \partial \rho = -\frac{N \partial x}{D_{i,j}^{eff}} \tag{11}$$

Where $D_{i,j}^{eff}$ is the effective diffusivity coefficient, which can be calculated from Slattery-Bird formula and Bruggemann correction:

$$\begin{aligned} D_{i,j} &= \frac{10.1325}{P_{tot}} a \left(\frac{T}{\sqrt{T_{crit,i} T_{crit,j}}} \right)^b \left(\frac{P_{crit,i} P_{crit,j}}{101325^2} \right)^{1/3} \\ &\times (T_{crit,i} T_{crit,j})^{5/12} \left(\frac{10^{-3}}{M_i} + \frac{10^{-3}}{M_j} \right)^{1/2} \end{aligned} \tag{12}$$

$$D_{i,j}^{eff} = D_{i,j} \times \varepsilon^{\xi} \tag{13}$$

Where $a = 3.64 \times 10^{-4}$ and $b = 2.334$ because H_2O is a polar gas. T_{crit} and P_{crit} are parameters depending on the gas type. P_{tot} is the total pressure of the gas.

The mass flows rate of the gas to the gas diffusion layer are directly related to fuel cell current:

$$N_{H_2} = i \frac{M_{H_2}}{2F} \tag{14}$$

$$N_{O_2} = i \frac{M_{O_2}}{4F} \tag{15}$$

$$N_{H_2O} = i \frac{M_{H_2O}}{2F} \tag{16}$$

Where M is the molar mass of the gas in $kg \cdot mol^{-1}$, i the fuel cell current in A and F is the Faraday constant.

III. Numeric solver scheme

In order to get a 2D pressure map in the channel with minimal calculation time, a one dimetional mass transfer model is used to calculate the pressur in channels. After that, the one dimentional map is interpolated to a two dimentional map (cf figure 1). Then, the medium pressur is calculated for the parametric calculation in electrochemical model.

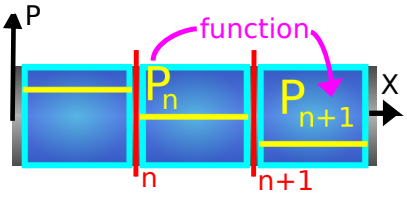

Fig. 2. One dimentional finit volume method recursive sequence illustration

A. Mass transfer solver scheme

1) 1D recurrent solver: The finit volume method is used to calculate variation of pressure in channels. The Figure 2 shows that the formulation can be explained as recursive sequence.

By using the Darcy-Weisbach's law, the perfect gas rule and the mass conservation, it is possible to set up the formulation:

$$P_{n+1} = P_n - f_{D_n}\rho_n \frac{dL}{D_h} \times \frac{u_n^2}{2} - \left(1 - \frac{\rho_n u_n S_{cha} - dQ}{\rho_n u_n S_{cha}}\right) P_n \tag{17}$$

With dL the size of the finite element in m and dQ is the mass flow per element in $kg \cdot s^{-1}$.

In order to use this formulation, it is needed to calculate other parameters in the respective order :

$$\rho_{n+1} = \frac{P_{n+1} M}{RT} \tag{18}$$

$$u_{n+1} = \frac{1}{\rho_{n+1} S_{cha}} \left(\rho_n u_n S_{cha} - dQ\right) \tag{19}$$

$$f_{D_n} = \frac{64\mu}{D u_{n+1} \rho_{n+1}} \tag{20}$$

Thus, the pressure is determined in a one dimensional matrix of Nb elements with the hypothesis of uniform diffusion : $dQ = \frac{N}{Nb \times Nb_{channel}}$

The dL parameter is determinate by :

$$dL = \frac{L_{channel}}{Nb} \tag{21}$$

Where Nb is the number of element in the one dimensional matrix.

For the anode side, the limit conditions are :

$$P_0 = P_{H_2,in} \tag{22}$$

$$u_0 = \frac{dQ Nb}{\rho_0 S_{cha}} \tag{23}$$

For the cathode side, an additive term for the O_2 concentration is added :

$$X_{n+1} = \frac{u_n \rho_n S_{cha} X_n - dQ}{u_{n+1} \rho_{n+1} S_{cha}} \tag{24}$$

The corresponding limit conditions are :

$$u_0 = \frac{u_{air,in}}{\rho_0 S_{cha}} \tag{25}$$

$$X_0 = 0.2 \tag{26}$$

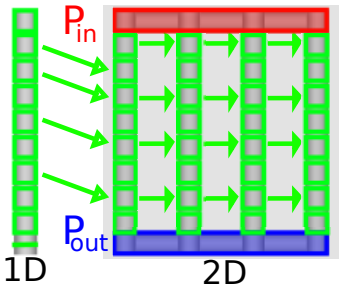

Fig. 3. Two dimensional pressure interpolation for parallel configuration

P_0 is the searching parameter to find $P_{Nb} = 1atm$ with a numerical dichotomy method. The $u_{air,in}$ is given by the empirical polynomial equation from the air compressor model of the fuel cell system :

$$\begin{aligned} u_{air,in} &= (6.04 \times 10^{-5} i^4 - 4.71 \times 10^{-3} i^3 \\ &\quad + 9.65 \times 10^{-2} i^2 + 1.05 i + 16.1) \times \tfrac{1.2}{60000}; \end{aligned} \tag{27}$$

2) 2D Pressure interpolation method:

a) Serial configuration: The channel is divide in Nb elements which have two dimensional position in (X,Y) surface. After that, the value of each part of the one dimensional matrice is put in its respective position of a two dimensional matrix as it is shown in the figure 1.

In order to calculate value between two positions, a linear interpolation is used :

$$P_b = \frac{L_{(X_1,Y_1)} P_{(X_2,Y_2)} + L_{(X_2,Y_2)} P_{(X_1,Y_1)}}{L_{(X_1,Y_1)} + L_{(X_2,Y_2)}} \tag{28}$$

With P_b the intermediate pressure to be determined, $P_{(X_1,Y_1)}$ and P_2 the respective pressures in position 1 and 2, $L_{(X_1,Y_1)}$ and L_2 the respective distance between position (X_1, Y_1) and position of P_b and position (X_2, Y_2) and position of P_b.

b) Parallel configuration: An hypothesis of uniform gas presence is taken for the pressure inlet and outlet part of the channel configuration with P_{in} and P_{out}. The $Nb_{parallel}$ channels are all calculate with same process like for serial as it is shown in the figure 3.

3) Average pressure in channel: The average gaz pressures are then calculated by :

$$P_{moy} = \frac{\sum P_n}{Nb} \tag{29}$$

IV. Results and Discussions

A. Model experimental validation

The developed 2D PEMFC has been validated experimentally by a Ballard NEXA 1.2 kW fuel cell stack of 47 cells. The fuel cell stack geometry and physical property parameters used in the model are listed in Table I.

The experimental and model predicted single cell polarization curve is shown in figure 4 for the entire fuel cell operating current range. It can be concluded from the figure that, the model shows a very good accuracy compared to the experimental results. In addition to the polarization curve,

TABLE I. BALLARD NEXA FUEL CELL STACK AND SIMULATION PARAMETERS

Parameter	Symbol	Value
Cell geometry		
Anode channel length	L_{H_2}	8.807e-1 m
Anode channel size	D_{H_2}	2.0e-3 m
Anode channel area	S_{cha,H_2}	4.0e-6 m^2
Anode channel perimeter	P_{cha,H_2}	8.0e-3 m
Anode channel number	$Nb_{channel,H_2}$	6
Cathode channel length	L_{air}	2.264 m
Cathode channel size	D_{air}	2.0e-3 m
Cathode channel area	$S_{cha,air}$	4.0e-6 m^2
Cathode channel perimeter	$P_{cha,air}$	8.0e-3 m
Cathode channel number	$Nb_{channel,air}$	2
Cell surface	A	1.4758e-2 m^2
Gas diffusion layer porosity	ε	0.45
Tortuosity	ξ	1.5
Gas diffusion layer thickness	δ_{GDL}	400e-6 m
Membrane thickness	δ_{mem}	200e-6 m
Butler and Volmer parameters		
Exchanging current	$i0_{ref}$	1.416 $A \cdot m^{-2}$
Symetry parameter	α	0.25
Number of electron exchanged	n	2
Cell operating conditions		
Hydrogen supply pressure	$P_{H_2,in}$	200000 Pa
Fuel cell temperature	T	333 K
Hydrogen wetness	H_{H_2}	90 %
Air wetness	H_{air}	70 %
Hydrogen dynamic viscosity	μ_{H_2}	9.3e-6 $Pa \cdot s$
Air dynamic viscosity	μ_{Air}	19.4e-6 $Pa \cdot s$
Physical Constant		
Perfect gas constant	R	8.314462 $J \cdot mol^{-1} \cdot K^{-1}$
Faraday constant	F	96474.70347 $C \cdot mol^{-1}$
Solver parameters		
Finite elements number	Nb	27
Parallel channels number	$Nb_{parallele}$	9

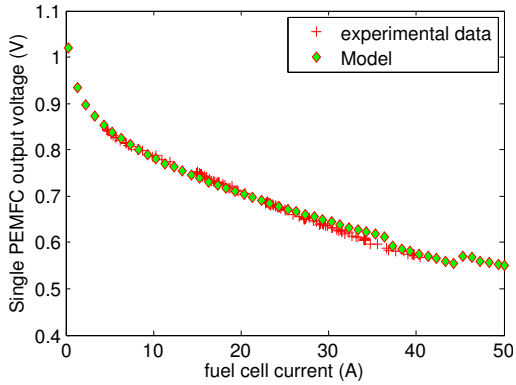

Fig. 4. Polarisation curve for one cell

the model experimental validation has also been made from different cell temporal current profiles of the 47 cell fuel cell stack.

The figure 5 show a very high dynamic current profiles of 300 seconds which is similar to a short fuel cell vehicle driving cycle. The measured fuel cells stack voltage and the model predicted voltage are shown and compared in figure 6. A very good agreement between the simulation and experimentation can be seen from the figure. For the whole time range, the maximum difference between the two curves is less than 10 % for a fuel cell stack of 47 individual cells.

A relatively low dynamic current profile is illustrated in figure 7. The stack voltages from both experimental and model are presented in figure 8. The model predicted values have a good agreement with the experimental one in general. A

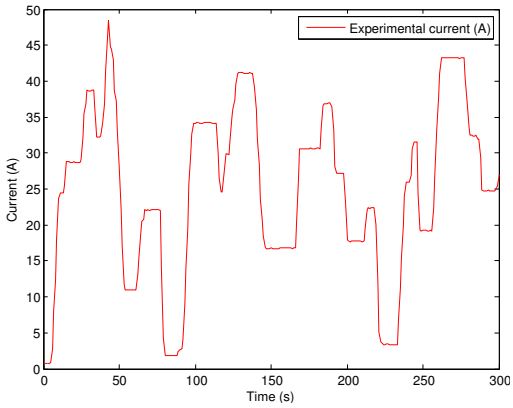

Fig. 5. Experimental validation with fast dynamic 1 (Current)

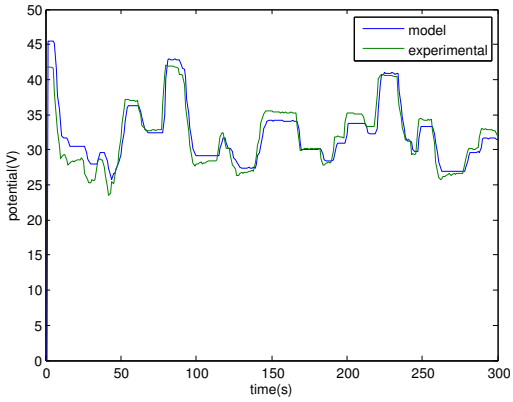

Fig. 6. Experimental Validation with fast dynamic 1

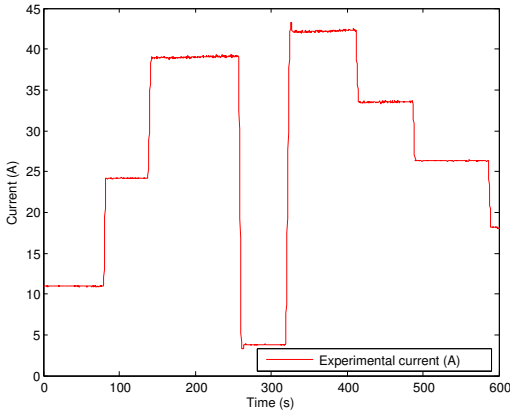

Fig. 7. Experimental Validation with slow dynamic 1 (Current)

slight difference can be observed at high current value. The possible reason for that difference is the over-estimation of the membrane water content in the developed model. In fact, for the real-time computation efficiency consideration, the membrane water content in the model is simply calculated from the average of the water activities of the anode and the cathode side. A more accurate nonlinear membrane water content model could be used in order to improve the water content estimation [14]. However the model real-time simulation capacity would be reduced in that case due to the complexity of the nonlinear model

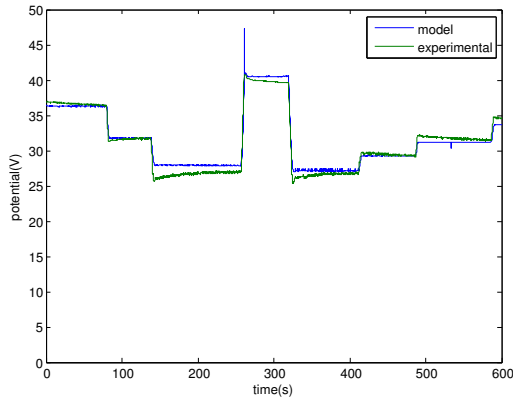

Fig. 8. Experimental Validation with slow dynamic 1

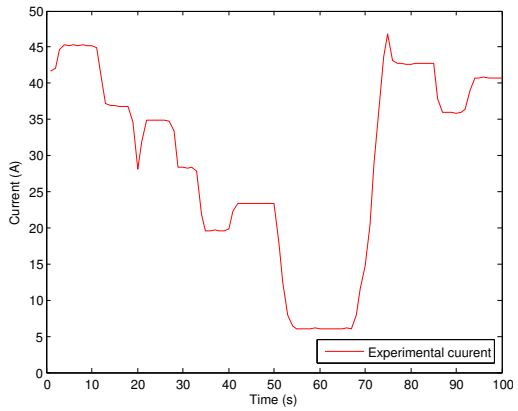

Fig. 9. Experimental Validation with fast dynamic 2 (Current)

Another current profile and the corresponding stack voltage from experimentation and simulation are shown in figure 9 and figure 10. The developed model shows a good agreement with the experimental results. A clear dynamic effect of the stack voltage can be seen from the experimental curve for constant current values. This dynamic is due to the fuel cell stack thermal capacity and the temperature variation during the operating [15]. This phenomenon cannot be reproduced from the current simulation, because the thermal dynamic of the fuel cell is not considered in the developed PEMFC model. Nevertheless, it can be seen from the figure that, the measured stack voltage converges closely to the steady-state model predicted value at the end of the thermal transient time.

A fourth current profile for model validation purpose is presented in figure 11. The figure 12 shows the model and experimental results for the fuel cell stack voltage. The results show again a good model accuracy of the model at different current values.

B. Reactant gas pressure in the channels

As described in the modeling section above, the developed 2D model is able to predict the channel pressure distribution for different gas supply channel geometry (serial and parallel configuration in particular). The Ballard NEXA fuel cell stack used for model experimental validation has serial channel geometry for anode hydrogen supply and parallel channel geometry for cathode air supply. From the model simulation,

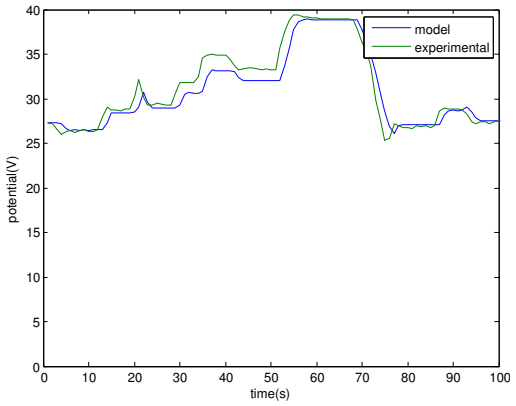

Fig. 10. Experimental Validation with fast dynamic 2

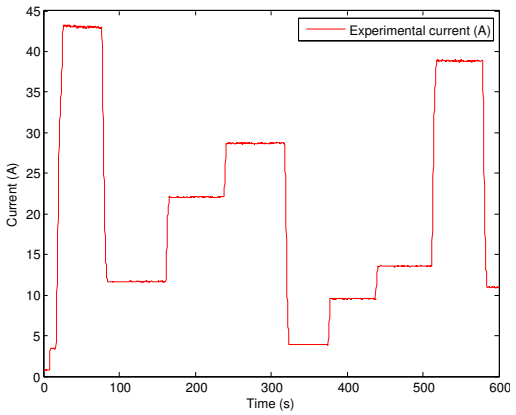

Fig. 11. Experimental Validation with slow dynamic 2 (Current)

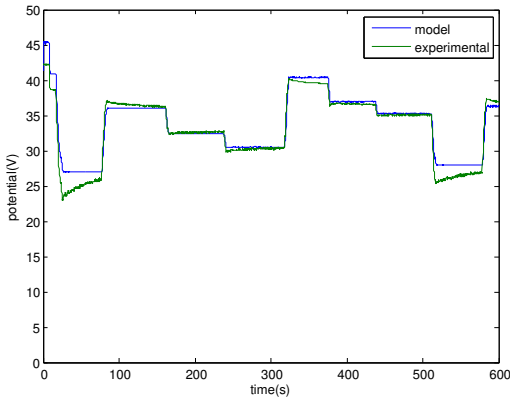

Fig. 12. Experimental Validation with slow dynamic 2

the corresponding gas pressure maps in the anode and cathode channels are also presented in the figure 13 and figure 14, respectively. It should be noted that the pressure value presented in figure 14 is the oxygen partial pressure in channel, which has a molar fraction of 21 % in the air. It can also be seen from the figures that, the pressure drop in the parallel channels is smaller compared to the serial one.

C. Practical efficiency modeling aspects

As it was explained, The main advantage of this modele is its abilit to work in real time. Its calculation time is very

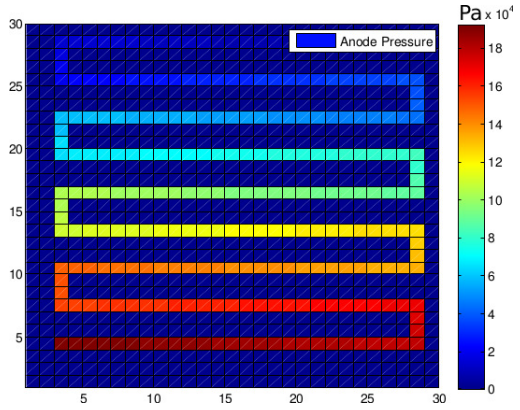

Fig. 13. Anode side channels pressure map (Pa)

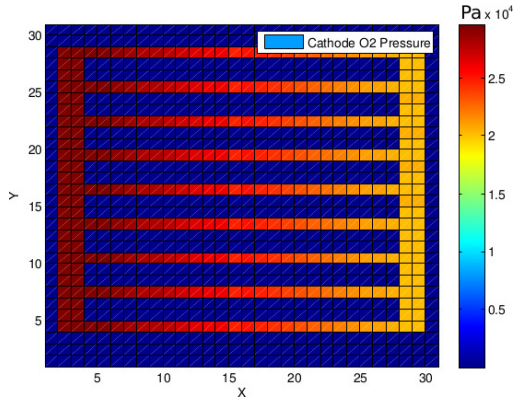

Fig. 14. Cathode side channels pressure map (Pa)

fast with less than 0.1s to calculate everything. But at the same time, it is not a one dimentional model, it gives a two dimentional pressure estimation matrix. The accurency of this numerical methode is medium low compare to usual numerical methode used in the models [3], [4] because the mistake rise with the channel longness.

Some ossilations can be seen on the polarisation curve fir hight current due to a begining of instabilities. The main aspect of this model is a compromise between fastness and stability which does not existe in other modeles [5] and [6].

V. Conclusion

In this paper, a real-time 2D PEMFC multiphysiques model has been developed. The fuel cell polarization curve, stack voltage temporal response for different current profiles and 2D gas pressure map for anode and cathode channels are presented and discussed. The developed model is validated experimentally with a commercial Ballard NEXA 1.2 kW fuel cell stack. The model predicted results show a very good accuracy compared with the experimental data. In order to improve the real-time simulation capacity of the model, a 1D to 2D numerical interpolation method has also been proposed to obtain the 2D gas pressure map in the cathode and the anode gas supply channel with the consideration of the different channel geometry configurations.

The presented real-time model is developed for a hybrid vehicle Hardware-in-the-Loop (HiL) application. In hybrid vehicle design, the fuel cell stack is usually combined with the supercapacitor and the battery. In our application, the fuel cell stack is operated around an operating point and the supercapacitor absorbs or provides the transient peak power demand during vehicle operation.

Improvement and future works include the consideration of nonlinear polymer membrane water content by modeling the electro osmotic drag and the back diffusion phenomena in the membrane and the expansion of the fluidic domain model to compare and estimate 2D gas distribution in different fuel cell components for design purpose.

References

[1] R. F. Mann, J. C. Amphlett, M. A. I. Hooper, H. M. Jensen, B. A. Peppley, and P. R. Roberge, "Development and application of a generalised steady-state electrochemical model for a pem fuel cell," *Journal of Power Sources*, vol. 86, pp. 173–180, 2000.

[2] F. Gao, B. Blunier, and A. Miraoui, *Modelisation de piles combustible membrane changeuse de protons*, Lavoisier, Ed. Kermes Science, 2011.

[3] R. M. Rao, D. Bhattacharyya, R. Rengaswamy, and S. Choudhury, "A two-dimensional steady state model including the effect of liquid water for a pem fuel cell cathode," *Journal of Power Sources*, vol. 1, pp. 375–393, 2007.

[4] M. Hu, A. Gu, M. Wang, X. Zhu, and L. Yu, "Three dimensional, two phase flow mathematical model for pem fuel cell: Part i. model development," *Energy Conversion and Management*, vol. 45, pp. 1861–1882, 2004.

[5] H. Meng, "A three-dimensional pem fuel cell model with consistent treatment of water transport in mea," *Journal of Power Sources*, vol. 162, pp. 426–435, 2006.

[6] M. A. R. S. Al-Baghdadi, "Three-dimensional computational fluid dynamics model of a tubular-shaped pem fuel cell," *Renewable Energy*, vol. 33, pp. 1334–1345, 2008.

[7] J. Baschuk and X. Li, "A general formulation for a mathematical pem fuel cell model," *Journal of Power Sources*, vol. 142, pp. 134–153, 2004.

[8] ——, "A comprehensive, consistent and systematic mathematical model of pem fuel cells," *Applied Energy*, vol. 86, pp. 181–193, 2009.

[9] G. N. Srinivasulu, T. Subrahmanyam, and V. D. Rao, "Parametric sensitivity analysis of pem fuel cell electrochemical model," *International Journal of Hydrogen Energy*, vol. 36, pp. 14 838–4844, 2011.

[10] R. Garca-Valverde, N. Espinosa, and A. Urbina, "Simple pem water electrolyser model and experimental validation," *International Journal of Hydrogen Energy*, vol. 37, pp. 1927–1938, 2012.

[11] C. Bao, M. Ouyang, and B. Yi, "Modeling and control of air stream and hydrogen flow with recirculation in a pem fuel cell system-i. control-oriented modeling," *International Journal of Hydrogen Energy*, vol. 141, pp. 96–101, 2005.

[12] F. Barbir, H. Gorgun, and X. Wang, "Relationship between pressure drop and cell resistance as a diagnostic tool for pem fuel cells," *Journal of Power Sources*, vol. 141, pp. 96–101, 2005.

[13] A. Rowe and X. Li, "Mathematical modeling of proton exchange membrane fuel cells," *Journal of Power Sources*, vol. 102, pp. 82–96, 2001.

[14] F. Gao, B. Blunier, A. Miraoui, and A. El-Moudni, "Cell layer level generalized dynamic modeling of a pemfc stack using vhdl-ams language," *International Journal of Hydrogen Energy*, vol. 34, no. 13, pp. 5498 – 5521, 2009.

[15] ——, "A multiphysic dynamic 1-d model of a proton-exchange-membrane fuel-cell stack for real-time simulation," *Industrial Electronics, IEEE Transactions on*, vol. 57, no. 6, pp. 1853–1864, 2010.